trialkylsiloxy nitroxide radicals have been obtained with nitromethane, nitroethane, and α-nitrotoluene.[47] Nitrobenzene absorbed too strongly at the excitation wavelength for the rate constant for its reaction with $Et_3Si\cdot$ radicals to be measured. However, our kinetic results with nitromethane show that the addition of $Et_3Si\cdot$ radicals to nitro groups is rapid. Nitro compounds should therefore make very effective spin traps for trialkylsilyl radicals.

Registry No. $Et_3Si\cdot$, 24669-77-0; $H_2C{=}CHC{\equiv}N$, 107-13-1; $H_2C{=}C(CH_3)C(O)OCH_3$, 80-62-6; $H_2C{=}CHC_6H_5$, 100-42-5; $H_2C{=}CCl_2$, 75-35-4; *trans*-$CH_3CH{=}CHC(O)OCH_3$, 623-43-8; $H_2C{=}CH_2$, 74-85-1; *cis*-$ClCH{=}CHCl$, 156-59-2; $Cl_2C{=}CCl_2$, 127-18-4; *trans*-$ClCH{=}CHCl$, 156-60-5; $H_2C{=}\overline{C(CH_2)_4C}H_2$, 1192-37-6; $H_2C{=}CH(CH_2)_3CH_3$, 592-41-6; $H_2C{=}CHC(CH_3)_3$, 558-37-2; $H\overline{C{=}CH(CH_2)_2C}H_2$, 142-29-0; $H\overline{C{=}CHO(CH_2)_2C}H_2$, 110-87-2; *trans*-$CH_3CH_2CH{=}CHCH_2CH_3$, 13269-52-8; $H\overline{C{=}CH(CH_2)_3C}H_2$, 110-83-8; $HC{\equiv}CC(CH_3)_3$, 917-92-0; $H_2C{=}C$, 536-74-3; $N{\equiv}CC(CH_3)_3$, 630-18-2; $N{\equiv}CC_6H_5$, 100-47-0; $C{\equiv}N(CH_2)_3CH_3$, 2769-64-4; $O{=}C{=}NC(CH_3)_3$, 1609-86-5; $C_6H_5CH{=}N(O)C(CH_3)_3$, 3376-24-7; O_2NCH_3, 75-52-5; triethylsilane, 617-86-7; benzene, 71-43-2; chlorobenzene, 108-90-7; toluene, 108-88-3; anisole, 100-66-3; 1-methylnaphthalene, 90-12-0; phenylacetylene, 536-74-3; pyridine, 110-86-1; pyrrole, 109-97-7; furan, 110-00-9; thiophene, 110-02-1; norbornadiene, 121-46-0.

Supplementary Material Available: Tables V–XXXVII, giving detailed kinetic data (25 pages). Ordering information is given on any current masthead page.

Models for Compounds I of Peroxidases: Axial Ligand Effects

Ichiro Fujita, Louise Karle Hanson, F. Ann Walker,[1] and Jack Fajer*

Contribution from the Department of Energy and Environment, Brookhaven National Laboratory, Upton, New York 11973, and the Department of Chemistry, San Francisco State University, San Francisco, California 94132. *Received July 26, 1982*

Abstract: A combination of model studies, theoretical calculations, and "in vivo" experiments has recently shown that ferryl porphyrin π cations provide viable models for the two-electron oxidation intermediates (compounds I) observed in the catalytic cycles of peroxidases and catalases. Extended Hückel calculations predict significant spin delocalization on the axial ligand, if an electron is abstracted from the a_{2u} orbital of the ferryl porphyrin. Similar profiles are computed for zinc porphyrins. Redox, optical, and ESR data are presented that probe the effect of bound pyridine on zinc cation radicals. The ESR results support the trend predicted by the calculations and provide evidence of spin density delocalization on the axial pyridine in a_{2u} radicals. Such axial delocalization in vivo may provide a conduit for electron exchange between the oxidized transients and neighboring protein residues. A mechanism is therefore proposed for the formation of compound ES of cytochrome *c* peroxidase in which reaction with peroxide leads to a transient ferryl-a_{2u} radical followed by electron transfer from an easily oxidized residue via the proximal histidine. Studies of a_{1u} zinc radicals indicate that complexation by nitrogenous ligands does not alter the ground-state occupancy and offer a reasonable explanation for the recent observation that compound I of horseradish peroxidase reconstituted with zinc protoporphyrin exhibits an optical spectrum similar to that of catalase.

Peroxidases and catalases are hemoprotein enzymes which decompose hydrogen peroxide in animals and plants[2,3] (catalase has recently been invoked[4] in photosystem II of green plants and may thus be involved in photosynthetic oxygen evolution). Three spectrally distinct transients, which lie two oxidation levels above the resting enzymes, have been observed on treatment of the ferrihemes with peroxide: the two green species typified by compounds I of horseradish peroxidase[5] (HRP) and bovine liver catalase[6] (CAT) or chloroperoxidase[7] (CPO), and the red compound ES of cytochrome *c* peroxidase[8] (CCP). Compounds I have been assigned to ferryl porphyrin π-cation radicals in which one oxidizing equivalent is stored in the form of a tetravalent iron stabilized by oxygen [$O{=}Fe^{IV}$] and the second equivalent resides in a porphyrin cation.[9-16] On the other hand, compound ES is described as a ferryl species with the second electron abstracted from a nearby protein residue.[8,17] On the basis of model studies

---

(1) San Francisco State University.

(2) Hewson, W. D.; Hager, L. P. "The Porphyrins"; Dolphin, D., Ed.; Academic Press: New York, 1978; Vol. 7, pp 295–332.

(3) Dunford, H. B.; Stillman, J. S. *Coord. Chem. Rev.* **1976**, *19*, 187–251.

(4) Nakatani, H. Y.; Barber, J. *Photobiochem. Photobiophys.* **1981**, *2*, 69–78. Barber, J.; Nakatani, H. Y.; Mansfield, R. *Isr. J. Chem.* **1981**, *21*, 243–249.

(5) Blumberg, W. E.; Peisach, J.; Wittenberg, B. A.; Wittenberg, J. B. *J. Biol. Chem.* **1968**, *243*, 1854–1862.

(6) Brill, A. S.; Williams, R. J. P. *Biochem. J.* **1961**, *78*, 253–262.

(7) Palcic, M. M.; Rutter, R.; Araiso, T.; Hager, L. P.; Dunford, H. B. *Biochem. Biophys. Res. Commun.* **1980**, *94*, 1123–1127.

(8) Yonetani, T.; Schleyer, H.; Ehrenberg, A. *J. Biol Chem.* **1966**, *241*, 3240–3247. Yonetani, T. *Enzymes, 3rd Ed.* **1976**, *13*, 345–361.

(9) (a) Dolphin, D.; Forman, A.; Borg, D. C.; Fajer, J.; Felton, R. H. *Proc. Natl. Acad. Sci.* U.S.A. **1971**, *68*, 614–618. (b) Dolphin, D.; Muljiani, Z.; Rousseau, K.; Borg, D. C.; Fajer, J.; Felton, R. H. *Ann. N. Y. Acad. Sci.* **1973**, *206*, 177–200. (c) Fajer, J.; Borg, D. C.; Forman, A.; Felton, R. H.; Vegh, L.; Dolphin, D. *Ibid.* **1973**, *206*, 349–364. (d) Felton, R. H.; Owen, G. S.; Dolphin, D.; Forman, A.; Borg, D. C.; Fajer, J. *Ibid.* **1973**, *206*, 504–515. (e) Fajer, J.; Borg, D. C.; Forman, A.; Adler, A. D.; Varadi, V. *J. Am. Chem. Soc.* **1974**, *96*, 1238–1239. (f) Felton, R. H. "The Porphyrins"; Dolphin, D., Ed.; Academic Press: New York, 1978; Vol. 5, pp 53–125. (g) Fajer, J.; Davis, M. S. "The Porphyrins"; 1979; Vol. 4, pp 197–256.

(10) (a) Loew, G. H.; Kert, C. J.; Hjelmeland, L. M.; Kirchner, R. F. *J. Am. Chem. Soc.* **1977**, *99*, 3534–3535. (b) Loew, G. H.; Herman, Z. S. *Ibid.* **1980**, 102, 6173–6174.

(11) Schultz, C. E.; Devaney, P. W.; Winkler, J.; Debrunner, P. G.; Doan, N.; Chiang, R.; Rutter, R.; Hager, L. P. *FEBS Lett.* **1979**, *103*, 102–105.

(12) Chin, D. H.; Balch, A. L.; LaMar, G. N. *J. Am. Chem. Soc.* **1980**, *102*, 1446–1448.

(13) Hager, L. P.; Doubek, D. L.; Silverstein, R. M.; Hargis, J. H.; Martin, J. C. *J. Am. Chem. Soc.* **1972**, *94*, 4364–4366.

(14) LaMar, G. N.; deRopp, J. S. *J. Am. Chem. Soc.* **1980**, *102*, 395–397. LaMar, G. N.; deRopp, J. S.; Smith, K. M.; Langry, K. C. *J. Biol. Chem.* **1981**, *256*, 237–243.

(15) Roberts, J. E.; Hoffman, B. M.; Rutter, R.; Hager, L. P. *J. Biol. Chem.* **1981**, *256*, 2118–2121; *J. Am. Chem. Soc.* **1981**, *103*, 7654–7656.

(16) Hanson, L. K.; Chang, C. K.; Davis, M. S.; Fajer, J. *J. Am. Chem. Soc.* **1981**, *103*, 663–670.

0002-7863/83/1505-3296$01.50/0

and theoretical calculations,[9,10,16] the spectral difference between compounds I of HRP and CAT or CPO has been ascribed to electron abstraction from one of two nearly degenerate highest occupied π orbitals of the porphyrins, the specific orbital, a_{1u} or a_{2u}, being determined by the proximal axial ligand of the heme.[9,16] In CAT and CPO which are ligated by tyrosine[18] and sulfhydryl[19] groups, respectively, oxidation is postulated[9,16] to occur from the a_{1u} orbital whereas in HRP, with a histidine ligand,[20] the electron is lost from the a_{2u} orbital.[21] Recent ^1H, ^2H, ^{14}N, and ^{17}O electron nuclear double resonance (ENDOR) results reported by Roberts et al.[15] support the ferryl-a_{2u} electronic profile predicted for compound I of HRP by the models and calculations.[9,16]

We extend here our previous work[9,16] to consider the effects of axial ligands on the spin densities of compounds I and test the theoretical calculations with ligated radicals of zinc porphyrins. Electron spin resonance (ESR) spectra establish that significant spin delocalization occurs onto the axial ligand in a_{2u} radicals, in agreement with the trend predicted by the calculations. Such axial delocalization may thus provide additional stabilization for porphyrin radical intermediates and also suggests a mechanism for coupling the radical to its protein environment. CCP could represent an extreme example of such an interaction in which compound ES would be preceded by a ferryl porphyrin π-cation followed by hopping of the hole on the cation to a protein residue situated near the proximal axial ligand.

Experimental and Theoretical Methods

ZnOEP[23] was prepared by reaction of zinc acetate with H_2OEP (Strem) in acetic acid, followed by chromatography on neutral alumina with CH_2Cl_2 and recrystallization from benzene. The syntheses of ZnTPrP,[9c] ZnTPP enriched with 95% ^{15}N[16] or 90% ^{67}Zn,[9c] ZnTPP-(D_{20}),[24] ZnTPP-py[25], and $(FeTPP)_2OClO_4$[26] have been described, as have the techniques used for ESR,[27] cyclic voltammetry[28] and controlled potential electrolyses.[24] The radicals used in the ESR experiments were generated in outgassed solutions by electron transfer[9c,27] to $(FeTPP)_2O$-ClO_4 ($E_{1/2}$ = 0.84 V vs. SCE in CH_2Cl_2[9d]).

The program and parameters used for the charge iterative extended Hückel (IEH) calculations have been described.[16,29,30] The geometry of the Zn coordination was based on the crystal structure of ZnTPP-py.[25b]

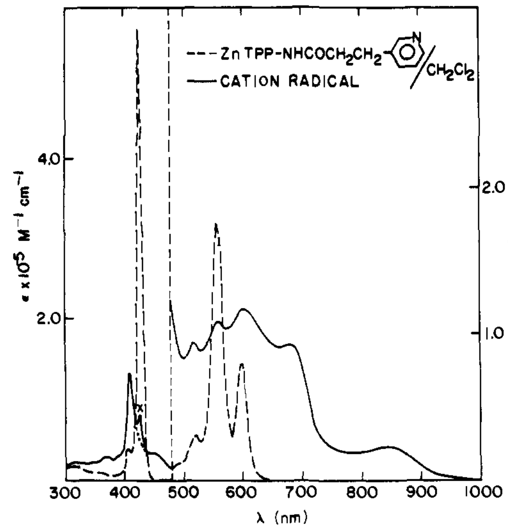

Figure 1. Optical absorption spectra, in CH_2Cl_2, of covalently bound ZnTPP-py (---) and its cation radical ZnTPP-py$^{+\cdot}$ [(—) x represents a small amount of unoxidized compound].

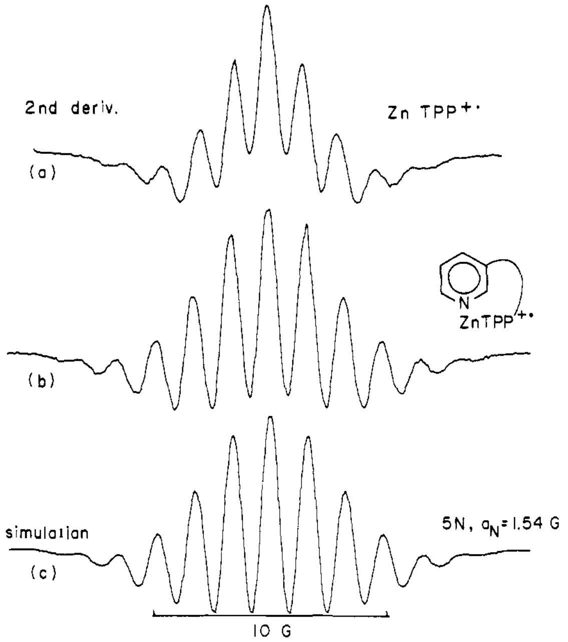

Figure 2. Second-derivative ESR spectra, in CH_2Cl_2, of (a) ZnTPP$^{+\cdot}$$ClO_4^-$ (g = 2.0026) and (b) ZnTPP-py$^{+\cdot}$$ClO_4^-$ (g = 2.0029). The simulation (c) demonstrates that five equivalent nitrogens determine the pattern observed in (b).

For the unpaired spin densities, ρ, given in Figure 6, the Zn was placed 0.37 Å out of plane, the ring center to pyrrole N distance was 2.025 Å, and Zn–pyridine N = 2.147 Å, with the pyridine eclipsing the pyrrole nitrogens. In the a_{2u} cation, decreasing Zn–N_{py} by 5% increased the unpaired spin densities on N_{py} and the ring nitrogens by ~1%. Lengthening the Zn–N_{py} bond by 10% resulted in a 15% increase in the calculated N_{py} spin with a 6% decrease in the $N_{pyrrole}$ densities. However, these effects probably result from a computational artifact: as the pyridine–Zn bond is weakened, a pyridine σ orbital is progressively raised in energy closer to the porphyrin a_{2u} (π), facilitating enhanced mixing between the two orbitals. Shortening Zn–Ct by 0.2 Å with the Zn–py and Ct-pyrrole distances kept fixed, increased with N_{py} spin density by 25% while the N(pyrrole) values remained the same. The a_{1u} calculations placed no unpaired spin density on the Zn or the axial pyridine; therefore, small changes in Zn geometry had no effect.

Results and Discussion

The salient features of a_{2u} cations are the localization of spin at the meso carbons and the nitrogens.[9c,e,g,10,16,24] To test the effect of a nitrogenous axial ligand on the electronic profile of a_{2u} cations, the redox, optical, and ESR parameters of several porphyrins were

---

(17) (a) Hoffman, B. M.; Roberts, J. E.; Brown, T. G.; Kang, C. H.; Margoliash, E. *Proc. Natl. Acad. Sci. U.S.A.* **1979**, *76*, 6132–6136. (b) Hoffman, B. M.; Roberts, J. E.; Kang, C. H.; Margoliash, E. *J. Biol. Chem.* **1981**, *256*, 6556–6564.

(18) Reid, T. J.; Murthy, M. R. N.; Sicignano, A.; Tanaka, N.; Musick, W. D. L.; Rossmann, M. G. *Proc. Natl. Acad. Sci. U.S.A.* **1981**, *78*, 4767–4771.

(19) Cramer, S. P.; Dawson, J. H.; Hodgson, K. O.; Hager, L. P. *J. Am. Chem. Soc.* **1978**, *100*, 7282–7290.

(20) Yonetani, T.; Yamamoto, H.; Erman, J. E.; Leigh, J. S.; Reed, G. H. *J. Biol. Chem.* **1972**, *247*, 2447–2455.

(21) The optical spectrum of compound I of human erythrocyte CAT differs from those of bovine liver or microbial catalases, and resembles an a_{2u} spectrum.[22] These results raise the possibility that the axial ligand of erythrocyte CAT is not tyrosine but may be a nitrogenous residue instead. Such a ligand would readily be detected in an ESR study of the Fe(II)nitrosyl complex, and the a_{2u} assignment could be tested by ENDOR experiments on compound I.

(22) Palcic, M. N.; Dunford, H. B. *J. Biol. Chem.* **1980**, *255*, 6128–6132.

(23) Abbreviations used for the porphinato dianions: OEP, 2,3,7,8,12,13,17,18-octaethyl; TPrP, 5,10,15,20-tetra-*n*-propyl; TPP, 5,10,15,20-tetraphenyl; TPP(D_{20}), 5,10,15,20-tetraperdeuteriophenyl; TPP-py, 5-[2-([2-(3-pyridyl)ethyl]carbonylamino)phenyl]-10,15,20-triphenyl. $(FeTPP)_2OClO_4$, perchlorate salt of the one-electron oxidation product of the μ-oxo dimer of Fe(III)TPP.

(24) Fajer, J.; Borg, D. C.; Forman, A.; Dolphin, D.; Felton, R. H. *J. Am. Chem. Soc.* **1970**, *92*, 3451–3459.

(25) (a) Walker, F. A.; Benson, M. *J. Am. Chem. Soc.* **1980**, *102*, 5530–5538. (b) Bobrik, M. A.; Walker, F. A. *Inorg. Chem.* **1980**, *19*, 3383–3390.

(26) Felton, R. H.; Owen, G. S.; Dolphin, D.; Fajer, J. *J. Am. Chem. Soc.* **1971**, *93*, 6332–6334.

(27) Borg, D. C.; Forman, A.; Fajer, J. *J. Am. Chem. Soc.* **1976**, *98*, 6889–6893.

(28) Fajer, J.; Brune, D. C.; Davis, M. S.; Forman, A.; Spaulding, L. D. *Proc. Natl. Acad. Sci. U.S.A.* **1975**, *72*, 4965–4960.

(29) Schaffer, A. M.; Gouterman, M.; Davidson, E. R. *Theor. Chem. Acta* **1973**, *30*, 9–30. Zerner, M.; Gouterman, M. *Ibid.* **1966**, *4*, 44–63. Zerner, M.; Gouterman, M.; Kobayashi, H. *Ibid.* **1966**, *6*, 363–400.

(30) Hanson, L. K. *Int. J. Quantum Chem., Quantum Biol. Symp.* **1979**, *6*, 73–87. Eaton, W. A.; Hanson, L. K.; Stephens, P. J.; Sutherland, J. C.; Dunn, J. B. R. *J. Am. Chem. Soc.* **1978**, *100*, 4991–5003.

Table I. Hyperfine Coupling Constants for Zinc Radicals with and without Axial Pyridine, in Gauss

compound	radical	radical plus pyridine
$ZnTPP^{+}\cdot(^{14}N)$	4 N, $a_N = 1.42$ G	5 N, $a_N = 1.54$ G[a]
$ZnTPP^{+}\cdot(^{15}N)$	4 N, $a_{^{15}N} = 1.99$ G	4 N, $a_{^{15}N} = 2.16$ G 1 N(py) $a_{^{14}N} = 1.54$ G
$^{67}ZnTPP^{+}\cdot(D_{20})$	4 N, $a_N = 1.42$ G 1 Zn, $a_{^{67}Zn} = 1.22$ G	5 N, $a_N = 1.54$ G 1 Zn, $a_{Zn} = 1.95$ G
$ZnTPrP^{+}\cdot$	4 N, $a_N = 1.68$ G 8 H (CH_2), $a_H = 2.75$ G	5 N, $a_N = 1.83$ G 8 H, $a_H = 2.82$ G
$ZnOEP^{+}\cdot$	not resolved, peak to peak line width of the first derivative signal, $\Delta H = 2.56$	not resolved, $\Delta H = 2.54$

[a] In $ZnTPP\text{-}py^{+}\cdot$ and $ZnTPP^{+}\cdot$ plus a 10-fold excess of py.

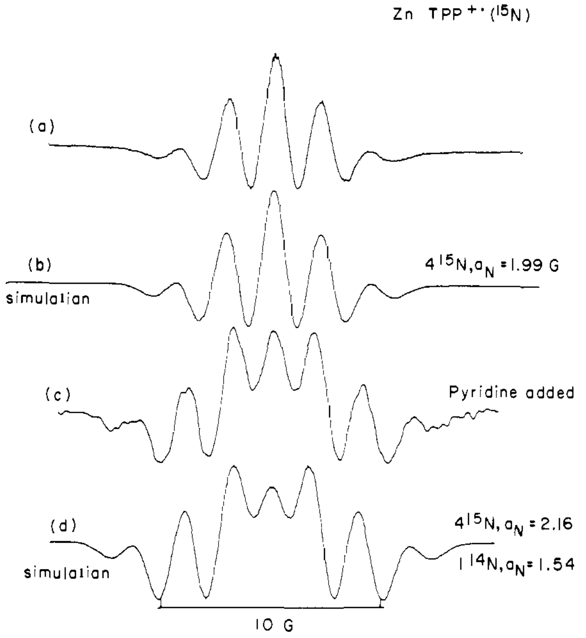

Figure 3. Second-derivative ESR spectra, in CH_2Cl_2, of (a) $ZnTPP^{+}\cdot(^{15}N)$ and (c) $ZnTPP^{+}\cdot(^{15}N)$ with pyridine(^{14}N) added. Simulation (b) assumes four nitrogens, $a_{^{15}N} = 1.99$ G; (d) includes four pyrrole nitrogens, $a_{^{15}N} = 2.16$ G and one pyridine nitrogen $a_{^{14}N} = 1.54$ G.

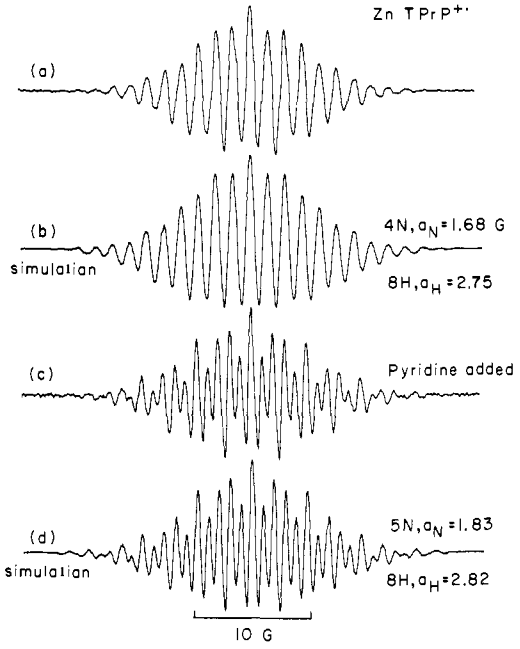

Figure 4. Second-derivative ESR spectra in CH_2Cl_2, of (a) $ZnTPrP^{+}\cdot$ and (c) $ZnTPrP^{+}\cdot$ with pyridine added. Simulation b includes four nitrogens and eight methylene protons; (d) incorporates five nitrogens and eight protons.

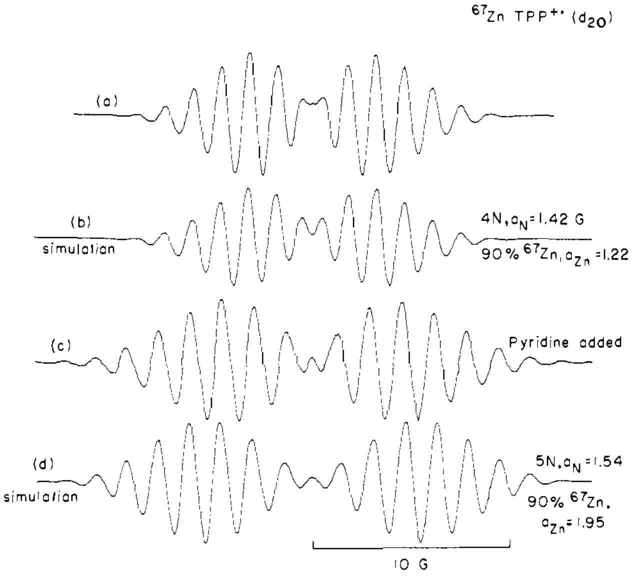

Figure 5. Second-derivative ESR spectra in CH_2Cl_2, of (a) $^{67}ZnTPP^{+}\cdot(D_{20})$ and (c) $^{67}ZnTPP^{+}\cdot(D_{20})$ with pyridine added (90% ^{67}Zn and deuterated phenyl groups. The deuteration minimizes the small contributions [$a_H \leq 0.3$ G] of the phenyl protons and yields better resolved spectra). Simulation d illustrates the increased spin density at the metal and nitrogens, as well as the additional nitrogen from the bound pyridine.

investigated. Initially, ZnTPP-py,[25] in which pyridine (py) is covalently bound, was chosen to avoid possible secondary reactions[31] of the radical with the excess pyridine needed[32,33] to completely complex ZnTPP in CH_2Cl_2. Controlled-potential oxidation[34] of ZnTPP-py requires 1 (±0.05) electron to yield the cation spectrum shown in Figure 1. The reaction is reversible: better than 95% of the parent compound is regenerated on reduction. The optical spectrum of $ZnTPP\text{-}py^{+}\cdot$ is analogous to that reported for $ZnTPP^{+}\cdot$ in the presence of large concentrations of py.[33] Whereas complexation of neutral ZnTPP by py causes significant shifts in the Soret and visible bands (5–15 nm),[25,32,33] the effects of ligation on the radical are minimal. The red and visible bands are comparable, with small changes in relative intensities while the Soret band red shifts by 2 nm relative to that of $ZnTPP^{+}\cdot$. The Soret band is, however, less intense in the ligated radical, $\epsilon_{411} = 1.35 \times 10^5\ M^{-1}\ cm^{-1}$, than in $ZnTPP^{+}\cdot$, $\epsilon_{409} = 1.9 \times 10^5\ M^{-1}\ cm^{-1}$.[24]

The presence of the py ligand is readily evident in the ESR spectrum of $ZnTPP\text{-}py^{+}\cdot$. Its 11-line spectrum (Figure 2) differs distinctly from the 9-line spectrum of $ZnTPP^{+}\cdot$ which arises[24] from interactions of the unpaired electron with the four equivalent nitrogens with $a_N = 1.42$ G. (The large spin density at the meso positions is obscured in TPPs because the phenyl groups lie out of the porphyrin plane.) The spectrum of $ZnTPP\text{-}py^{+}\cdot$ can be assigned to *five* equivalent nitrogens with $a_N = 1.54$ G by computer simulation[35] (Table I). To ensure that the additional nitrogen

---

[31] In acetonitrile, py attacks $ZnTPP^{+}\cdot$ at the β pyrrole position. Shine, H. J.; Padilla, A. G.; Wu, S. M. *J. Org. Chem.* **1979**, *44*, 4069–4075.

[32] Nappa, M.; Valentine, J. S. *J. Am. Chem. Soc.* **1978**, *100*, 5075–5080.

[33] Kadish, K. M.; Shine, L. R.; Rhodes, R. K.; Bottomley, L. A. *Inorg. Chem.* **1981**, *20*, 1274–1277.

[34] Pyridine ligation has little effect on the oxidation potential of ZnTPP. The half-wave oxidation potential of ZnTPP-py is 0.72 V to be compared with 0.76 V for the bare ZnTPP (vs. SCE in CH_2Cl_2 containing 0.1 M tetrapropylammonium perchlorate). This value is similar to that reported[33] for ZnTPP in CH_2Cl_2 containing 1 M py: $E_{1/2} = 0.76$ V. Anionic ligands induce a more pronounced effect by stabilizing the charge on the radical. For example, addition of chloride to ZnTPP causes optical changes parallel to those observed with py but the complex is easier to oxidize by almost 0.2 V.[9c]

[35] The simulations neglect the small coupling constants of ~0.3 G due to the protons of the phenyl groups in $ZnTPP^{+}\cdot$.[24] These are subsumed in the line widths used in the simulations. Line width and line shape variations introduce an ~3% spread in the coupling constants reported.

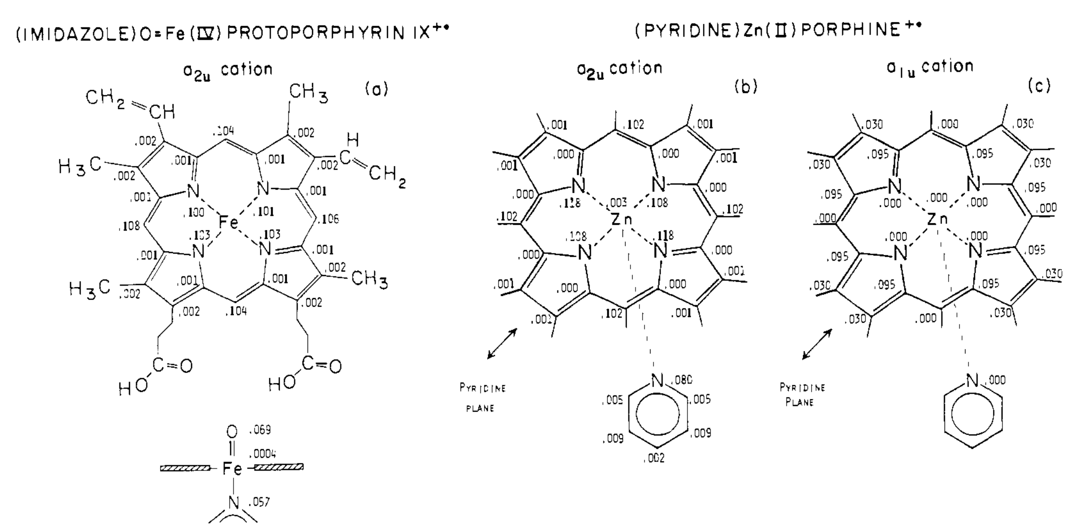

Figure 6. Calculated unpaired spin densities, ρ: (a) $S = {}^3/_2$ ferryl protoporphyrin IX a_{2u} π-cation radical with an imidazole ligand[16] (a model for compound I of HRP and the proposed transient in CCP). In a series of ferryl *porphine* radicals ligated by imidazole, hydrogen-bonded imidazole, and imidazolate, ρ at the nitrogen bonded to the iron increases from 0.055 to 0.061 to 0.091, respectively. The densities at the oxygen increase similarly from 0.066 to 0.070 to 0.121. All values shown represent the contributions from the a_{2u} π orbitals. (b) Pyridine-bound zinc porphine a_{2u} cation. (c) Pyridine-bound zinc porphine a_{1u} cation. In (b) shorter Ct–Zn and/or longer Zn–py distances increase the spin density at the py nitrogen and therefore tend to equalize ρ at the nitrogens of the pyrroles and the pyridine (see Experimental and Theoretical Methods). In (c), small variations in the coordination of the Zn have no effect.

interaction did not result from overlap of the amide in the linking chain[25] with the high spin density at the 5-meso position, ZnTPP was oxidized in the presence of a 10-fold excess of py. The resulting ESR spectrum is identical with that of ZnTPP-py$^{+\cdot}$ and clearly establishes that the fifth nitrogen interaction arises from the ligand. This assignment can be further verified by examining the spectrum of ^{15}N ZnTPP$^{+\cdot}$. Because of the different nuclear spin ($I = {}^1/_2$) and gyromagnetic ratio of ^{15}N, the spectrum of ZnTPP$^{+\cdot}$(^{15}N) consists[16] of five lines with $a_{^{15}\mathrm{N}} = 1.99$ G (Figure 3a,b). On addition of py a seven-line spectrum is observed (Figure 3c,d), which reflects the coupling constant of the py nitrogen, $a_{^{14}\mathrm{N}} = 1.54$ G derived from the ZnTPP-py$^{+\cdot}$ spectrum and the ^{15}N constants of the porphyrin which have now increased by 8% (as in ZnTPP-py$^{+\cdot}$) to $a_{^{15}\mathrm{N}} = 2.16$ G.

A similar effect is observed with ZnTPrP$^{+\cdot}$ in the presence of pyridine. In addition, this compound allows the spin density at the meso positions to be sampled via the methylene coupling constants. As shown in Figure 4, the ESR spectrum of ZnTPrP$^{+\cdot}$, which arises from the four pyrrole nitrogens ($a_\mathrm{N} = 1.68$ G) and the eight methylene protons ($a_\mathrm{H} = 2.75$ G),[36] changes, on addition of pyridine, to a new spectrum caused by eight protons ($a_\mathrm{H} = 2.82$ G) and five nitrogens ($a_\mathrm{N} = 1.83$ G). The meso positions thus remain effectively unperturbed while the splittings of the pyrrole nitrogens have increased by 9%, and the pyridine nitrogen bears a comparable coupling constant, as in ZnTPP-py$^{+\cdot}$.

If spin delocalization onto the axial ligand occurs, the question then arises: What happens to the metal itself? The spectrum of ^{67}ZnTPP(D$_{20}$)$^{+\cdot}$ (90% ^{67}Zn, $I = {}^5/_2$) is displayed in Figure 5 along with a simulation which assumes[9c] four nitrogens, $a_\mathrm{N} = 1.42$ G and one zinc, $a_{^{67}\mathrm{Zn}} = 1.22$ G. [Allowances have been made for the 10% of ZnTPP(D$_{20}$)$^{+\cdot}$.] On addition of py, a broader spectrum is observed which can be fitted to five nitrogens, $a_\mathrm{N} = 1.54$ G (as in ZnTPP-py$^{+\cdot}$) and $a_{^{67}\mathrm{Zn}} = 1.95$ G (Figure 5). The metal coupling constant has thus increased ~60% but is still very small.[37] Although X-ray data indicate[38] that oxidation has little effect on the displacement of the zinc from the plane of the four nitrogens in ZnTPP$^{+\cdot}$ClO$_4^-$ and that the displacements are comparable[25b] in ZnTPP$^{+\cdot}$ and neutral ZnTPP-py, the increase in spin density at the zinc could conceivably result from a small variation in the geometry of the metal.[39]

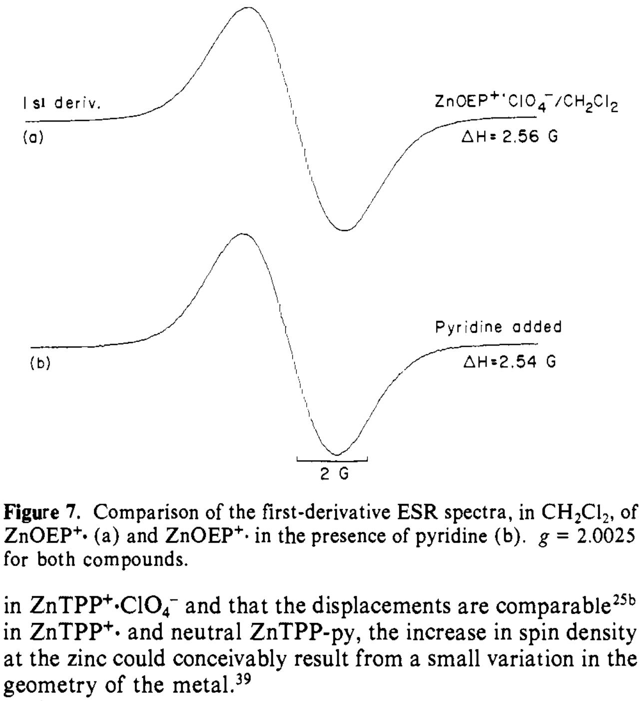

Figure 7. Comparison of the first-derivative ESR spectra, in CH$_2$Cl$_2$, of ZnOEP$^{+\cdot}$ (a) and ZnOEP$^{+\cdot}$ in the presence of pyridine (b). $g = 2.0025$ for both compounds.

These data establish that complexation of an a_{2u} radical by a nitrogenous ligand such as pyridine results in an ~10% increase in the pyrrole nitrogen coupling constants accompanied by a significant interaction with the nitrogen atom of the ligand via the metal.[40] Such a profile, i.e., high spin densities at the meso positions, the pyrrole nitrogens, *and* the nitrogen of the axial ligand, is indeed predicted by IEH calculations for ligated zinc radicals as well as for compound I of HRP[16] (Figure 6). The agreement between the experimental results and the calculations for the zinc radicals lends credence to the calculations for HRP I and suggests therefore that the ^{14}N ENDOR coupling constants detected by Roberts et al.[15] in HRP I include contributions from the imidazole bound to the heme radical.[41]

---

(36) The methylene assignments have been confirmed by selective deuterations (unpublished results). The coupling constants are approximately half those predicted by calculations or those observed in the meso tetramethyl homologue because of restricted rotation of the methylene groups.[9c,g]

(37) The isotropic hyperfine coupling for an electron localized on ^{67}Zn is reported as 446 G. Wertz, J. E.; Bolton, J. R. "Electron Spin Resonance. Elementary Theory and Practical Applications"; McGraw-Hill: New York, 1972.

(38) Spaulding, L. D.; Eller, P. G.; Bertrand, J. A.; Felton, R. H. *J. Am. Chem. Soc.* **1974**, *96*, 982–987.

(39) We assume that ZnTPP-py$^{+\cdot}$ClO$_4^-$ is pentacoordinated with the perchlorate ion positioned on the side as in Fe(III)TPPCl$^{+\cdot}$SbCl$_6^-$: Gans, P.; Marchon, J. C.; Reed, C. A. *Nouv. J. Chim.* **1981**, *5*, 203–204.

(40) A similar increase in the pyrrole nitrogens and delocalization onto the axial ligand has also been observed in a_{2u} radicals complexed by halide ions.[9c,e,g]

In contrast to the spin density profile observed in a_{2u} radicals, model studies and calculations indicate[9,16] a very different spin distribution for a_{1u} radicals (Figure 6). Most of the unpaired spin is localized at the α-carbons of the pyrroles with $a_{\mathrm{N}_{\mathrm{pyrrole}}} < 0.3$ G and $a_{\mathrm{H}_{\mathrm{meso}}} = 1.2$–1.5 G (in typical a_{1u} radicals such as ZnOEP$^{+\cdot}$, MgOEP$^{+\cdot}$, and zinc tetrabenzporphyrin$^{+\cdot}$).[9,16] Addition of complexing anions such as Cl$^-$ or Br$^-$ has little effect on the ESR spectra of ZnOEP$^{+\cdot}$.[9c] Similarly, as shown in Figure 7, addition of py to ZnOEP$^{+\cdot}$ does not alter the singlet ESR spectra within the limits of detection (peak to peak line widths of the first derivative spectra = 2.54–2.56 G).[42] The optical spectrum of ZnOEP$^{+\cdot}$ is characteristic of a_{1u} radicals[9b] and provides a rationale for the interesting observation[43] that oxidation of HRP reconstituted with zinc protoporphyrin (ZnProtoP) leads to a free radical species with an optical spectrum similar to that of compound I of CAT (a_{1u})[16] rather than of HRP (a_{2u}).[16] If ZnOEP is taken as a viable model for ZnProtoP, and since py ligation of ZnOEP$^{+\cdot}$ does not alter its ground-state occupancy,[44] we assign the zinc-reconstituted HRP radical to an a_{1u} species as well and thus can offer a simple explanation for its CAT-like absorption spectrum.

The reconstitution results further reinforce the notion, already amply demonstrated by a variety of other techniques,[9–16] that at least one oxidizing equivalent of HRP I is stored in the form of a porphyrin π cation and *not* as an oxidized protein residue, an alternative frequently considered.[2,3,14,46] This controversy has been fueled, in part, by the observations that compound ES of CCP, which also lies two oxidation levels above the resting enzyme, does exhibit a narrow ESR signal, ENDOR features, Mössbauer parameters, and optical spectra consonant with a ferryl porphyrin *and* a residue radical.[2,3,8,17,47] This overall oxidation level seems to be equivalent to the one which results from the reaction of HRP I with a substrate, S, to yield compound II:

$$\mathrm{O{=}Fe^{IV}P^{+\cdot}(HRP\ I) + S \rightarrow O{=}Fe^{IV}P(HRP\ II) + S^{+\cdot}}$$

It is attractive to speculate therefore that a ferryl porphyrin cation transient is common to all peroxidases and catalases on reaction with peroxides and that the distinguishing feature of CCP is the presence of an oxidizable residue R which acts as an indigenous substrate and reduces the porphyrin radical to yield compound ES:

$$\mathrm{Fe^{III}P^{+} + H_2O_2 \rightarrow O{=}Fe^{III}P^{+\cdot} + H_2O}$$

followed by

$$\mathrm{O{=}Fe^{IV}P^{+\cdot} + R \rightarrow O{=}Fe^{IV}P + R^{+\cdot}}$$

Possible candidates for R have variously been postulated as tryptophan-51 on the distal side of the heme[48] or methionine-172, coupled to another residue, on the proximal side.[17] Since the proximal ligand of the CCP heme is a histidine,[49] the putative ferryl π-cation of CCP would therefore be an a_{2u} cation,[16] with spin density on the imidazole, if the extrapolation from the theoretical and experimental results presented above is valid. This delocalization of spin on the *proximal side* would place the methionine within 4 Å of the heme radical,[50] a distance conducive to rapid electron transfer.[51] The oxidized methionine radical could be further stabilized[17] by a neighboring aspartate residue[50] and thereby provide a pathway for the electron flow that eventually results in the oxidation of cytochrome *c*, the physiological substrate of CCP.

The same electron-transport mechanism would apply to the transfer of the second oxidizing equivalent *if* the ferryl species remaining after consumption of the first equivalent is assumed to protonate and undergo an internal electronic isomerization[8] to yield a hydroxy ferri-π cation:

$$\mathrm{O{=}Fe^{IV}P \xrightarrow{H^+} HO{-}Fe^{IV}P^{+} \rightleftharpoons HO{-}Fe^{III}P^{+\cdot}}$$

Unlike the ferryl species, in which spin density is localized on the iron and oxygen atoms,[16] the Fe(III) radical would possess an electronic profile similar to that of the original ferryl π-cation.

Note Added in Proof. The effects of nitrogenous ligands on a_{2u} radicals have been extended to include imidazole (Im), a better model for the proximal histidines of HRP and CCP. At room temperature, Im reduces ZnTPP$^{+\cdot}$ immediately. The ZnTPP–Im$^{+\cdot}$ complex can be stabilized at −50 °C and exhibits an optical spectrum similar to the one shown in Figure 1. Its 11-line ESR spectrum resembles that of ZnTPP–py$^{+\cdot}$ and can be assigned, based on results obtained for ^{14}N and ^{15}N ZnTPP–Im$^{+\cdot}$, to four pyrrole nitrogens, $a_{^{14}\mathrm{N}} = 1.65$ (±0.05) G, and one Im nitrogen, $a_{\mathrm{N}} = 1.80$ (±0.05) G, to be compared with $a_{\mathrm{N}} = 1.50$ (±0.05) G for ZnTPP$^{+\cdot}$ and an average a_{N} value of 1.62 (±0.05) G for the five nitrogens of ZnTPP–py$^{+\cdot}$ at the same temperature.

Acknowledgment. We thank Dr. Thomas Poulos for a valuable discussion. This work was supported by the Division of Chemical Sciences, U.S. Department of Energy, under Contract No. DE-AC02-75CH00015, at Brookhaven National Laboratory and by grants from the National Science Foundation (CHE79-18217) and the National Institutes of Health (RCDA 5K04 GM 00227) at San Francisco State University.

Registry No. ZnTPP$^{+\cdot}$(^{14}N), 39732-73-5; ZnTPP$^{+\cdot}$(^{15}N), 84959-56-8; ^{67}ZnTPP$^{+\cdot}$(D$_{20}$), 84959-57-9; ZnTPrP$^{+\cdot}$, 51223-16-6; ZnOEP$^{+\cdot}$, 39586-99-7; ZnTPP$^-$py$^{+\cdot}$, 84959-58-0; HRP, 9003-99-0; CCP, 9029-53-2.

---

(41) To date, the major features of the calculations for HRP I[16] are in good agreement with experimental NMR[14] and ENDOR[15] results for the pyrrole nitrogens,[15] the oxygen of the ferryl moiety[15] and the substituents at the β positions of the pyrroles.[14,15] A reviewer has requested that we also test the calculations by comparing an a_{2u} zinc radical with and without py. For ZnP$^{+\cdot}$ClO$_4^-$, with the counterion positioned as observed[38] in the X-ray structure of ZnTPP$^{+\cdot}$ClO$_4^-$, the ρ values are 0.121 at the meso positions, 0.110 and 0.111 at the pyrrole nitrogens, and 0.016 at the zinc to be compared with values of 0.102 (meso), 0.108 and 0.118 (pyrrole nitrogens), and 0.003 (Zn) for the pyridine complex (from Figure 6). As discussed above, the experimental results for the two types of radicals show the coupling constants to be essentially unchanged at the meso positions and to have increased by ~10% at the pyrrole nitrogens and by ~60% at the zinc. Since the observed coupling constant of the latter is very small and since the origin of the metal hyperfine coupling in Zn radicals has been attributed to a σ–π polarization mechanism (Mengersen, C.; Subramanian, J.; Fuhrhop, J. H.; Smith, K. M. *Z. Naturforsch, A* **1974**, *29A*, 1827–1833), any small movement of the Zn should result in a large change in its observed coupling. The decrease of ~20% at the meso positions is not observed experimentally, but here again, conformational changes may influence the observed splittings. (For example, the X-ray structure of ZnTPP$^{+\cdot}$ClO$_4^-$ shows the macrocycle to be puckered.) The observed increase in the pyrrole nitrogen splittings does follow the trend predicted by the calculations and, more significantly, so does the axial ligand. The salient features of the spin density profiles predicted by the calculations for the two radicals are certainly observed experimentally.

(42) That the py is ligated to ZnOEP is evident from the red shifts in the optical spectrum $\lambda_{\max} = 566$, 529, and 400 nm vs. 575, 539, and 412 nm and the cathodic shift in the oxidation potential, $E_{1/2} = 0.67$ V for ZnOEP to 0.59 V for the complexed species.

(43) Kaneko, Y.; Tamura, M.; Yamazaki, I. *Biochemistry* **1980**, *19*, 5795–5799.

(44) ZnOEP-py absorbs at 575, 539, and 412 nm to be compared with maxima at 588, 551, and 426 for ZnProtoP in pyridine.[43] Attempts at obtaining an optical spectrum of ZnOEPpy$^{+\cdot}$ were complicated by the formation of its dimer (ZnOEPpy)$_2^{2+}$. The spectrum of the monomer is nonetheless similar to that of ZnOEP$^{+\cdot}$ and clearly a_{1u}. The dimer is diamagnetic and does not interfere with the ESR measurements.[9b,45] Since the dimerization requires that two positively charged species join, the process is favored by increasing solvent polarity[45] and, apparently, by complexing agents as well: whereas ZnOEP$^{+\cdot}$ is monomeric in CH$_2$Cl$_2$, addition of py yields a large fraction of the dimer. Similar results are obtained with a derivative in which py is covalently bound. Details of these results will be presented elsewhere.

(45) Fuhrhop, J. H.; Wasser, P.; Riesner, D.; Mauzerall, D. *J. Am. Chem. Soc.* **1972**, *94*, 7996–8001.

(46) Morishima, I.; Ogawa, S. *J. Am. Chem. Soc.* **1978**, *100*, 7125–7127; *Biochem. Biophys. Res. Commun.* **1978**, *83*, 946–953; *Biochemistry* **1978**, *17*, 4384–4388.

(47) Simonneaux, G.; Scholz, W. F.; Reed, C. A.; Lang, G. *Biochim. Biophys. Acta* **1982**, *716*, 1–7.

(48) Poulos, T. L.; Kraut, J. *J. Biol. Chem.* **1980**, *255*, 8199–8205; "From Cyclotrons to Cytochromes", Kaplan, N. O.; Robinson, A.; Eds.; Academic Press: New York, 1982, pp 193–201.

(49) Poulos, T. L.; Freer, S. T.; Alden, R. A.; Edwards, S. L.; Skogland, U.; Tako, K.; Eriksson, B.; Xuong, N.; Yonetani, T.; Kraut, J. *J. Biol. Chem.* **1980**, *255*, 575–580.

(50) Poulos, T. L., personal communication.

(51) Fujita, I.; Fajer, J.; Chang, C. K.; Wang, C. B.; Bergkamp, M. A.; Netzel, T. L. *J. Phys. Chem.* **1982**, *86*, 3754–3759.